

Assembly of lightweight sandwich panels through joining by forming

RFV Sampaio¹, JPM Pragana¹, IMF Bragança², CMA Silva¹ and PAF Martins¹ 

Proc IMechE Part L
J Materials: Design and Applications
 2021, Vol. 235(7) 1645–1654
 © IMechE 2021
 Article reuse guidelines:
sagepub.com/journals-permissions
 DOI: 10.1177/1464420721999827
journals.sagepub.com/home/pil



Abstract

This paper is focused on the assembly of lightweight sandwich panels built upon the patented ‘Opencell’ structure concept. The objective is to investigate the possibility of joining the connection members of the core to the adjoining skin sheet by plastic deformation at ambient temperature, instead of welding or adhesive bonding. The methodology draws from earlier developments of the authors in joining by forming using the mortise-and-tenon concept to experimentation and finite element modelling of the assembly process in unit cells that are representative of the sandwich panels. It is shown that replacing welding by joining by forming allows fabricating sandwich panels from sheet materials that are difficult or impossible to weld while preventing thermal cycles that are responsible for causing metallurgical changes, distortions, and residual stresses. Replacing adhesive bonding by joining by forming circumvents the need of surface preparation, time for the adhesive to cure and environmental compliance, among other requirements.

Keywords

Sandwich panels, metals, composites, joining by forming, experimentation, finite element method

Date received: 14 February 2021; accepted: 14 February 2021

Introduction

The exploitation of the economic advantages of weight reduction has been giving rise to a growing demand of lightweight sandwich panels for packaging, thermal and acoustic insulation, energy-absorbing applications, structural construction, and furniture. Lightweight sandwich panels are generally made of three-layer arrangements consisting of a central layer (core) and two solid material surface layers (skin sheets).

The core is responsible for supporting the skin sheets and preventing their movement (both in-plane and out-of-plane) whereas the skin sheets are responsible for carrying the normal and shear stresses. As a result of this, the selection and optimization of the material and geometry of the core and skin sheets according to the requirements of each specific application permits constructions to achieve physical, chemical, and mechanical performances that are far beyond what is achievable with conventional monolithic materials.

A possible classification of lightweight sandwich panels is based on how the task of supporting the skin sheets is fulfilled by the different types of cores.¹ Five different categories are identified (Figure 1): (i) sandwich panels with polymer or

foam cores, (ii) sandwich panels with pin cores, (iii) sandwich panels with corrugated cores, (iv) sandwich panels with cup-shaped cores and (v) sandwich panels with honeycomb cores.

Sandwich panels with polymer or porous cellular cores are typically made from polyamide and/or polyethylene sheets or from polyurethane or polypropylene foams that are glued to the skin sheets.^{2,3} The main advantages of these panels are the low weight (due to the low density of the core), low cost, and the homogeneous support of the skin sheets.

Sandwich panels with pin cores deliver good strength and stiffness performances with a reduced core weight.⁴ However, the pins are only able to provide (non-homogeneous) punctual support of the skin sheets and their positioning angle has a major influence on the balance between the shear and compression properties of the panels.

¹IDMEC, Instituto Superior Técnico, Universidade de Lisboa, Portugal

²CIMOSM, Instituto Superior de Engenharia de Lisboa, Instituto Politécnico de Lisboa, Portugal

Corresponding author:

PAF Martins, Instituto Superior Técnico, Universidade de Lisboa, Av. Rovisco Pais, Lisbon 1049-001, Portugal.

Email: pmartins@tecnico.ulisboa.pt

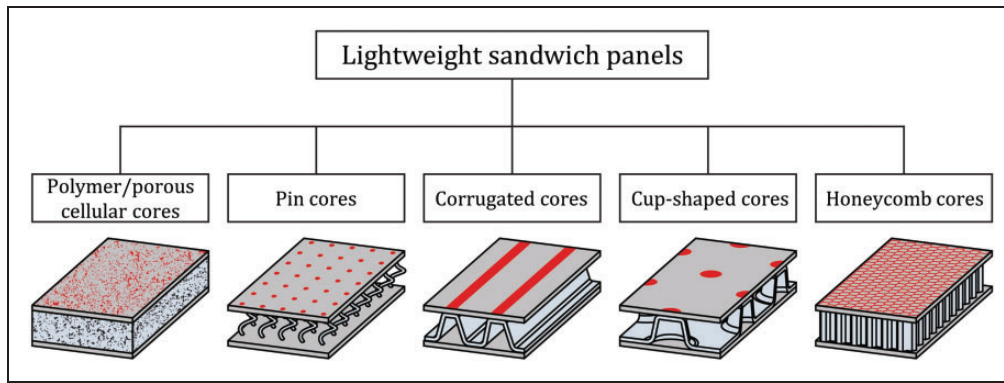


Figure 1. Classification of lightweight sandwich panels as a function of the skin sheet support provided by the different types of cores.

Sandwich panels with corrugated cores are widely used in cardboard packaging as well as in automotive and building applications. Their cores are made of triangular, trapezoidal, or sinusoidal cells open to one side, which provide unidirectional (heterogeneous) support of the skin sheets and are responsible for the significant differences in strength and stiffness in the longitudinal and transverse directions.⁵ The overall level of heterogeneity and the corresponding differences in mechanical performance can be diminished by using cut-shaped cores with cells open to both sides, which provide bidirectional support spots of the skin sheets.

Sandwich panels with honeycomb (uniform hexahedral) cores are made of vertical cells that open in the thickness direction to provide bi-directional support of the skin sheets. They are characterized by high strength and stiffness performances per weight, offering great potential for material savings⁶ but they are costlier and more difficult to fabricate than the sandwich panels with corrugated or cup-shaped cores.

In case of all-metal sandwich panels⁷ that will be the subject of this paper, recent developments towards the utilization of lattice truss core structures capable of providing bi-directional support of the skin sheets led to the development of an innovative structure concept called Opencell.^{8,9} In the Opencell concept, the core is built upon connection members that are formed (cut and bended) from the adjoining skin sheets, without the need of extra materials (Figure 2). This allows tailoring the design and number of the connection members in the core to achieve balanced (quasi-homogeneous) strength and stiffness responses in the longitudinal and transverse directions with significant weight savings.

However, the assembly of sandwich panels based on the Opencell structure concept through welding (Figure 2(a)) is a critical issue in the overall manufacturing route because welding (e.g. laser, resistance spot welding, or gas metal arc welding) requires the adjoining sheets to be made from similar

materials. Otherwise, there is a risk of incidence of hard and brittle intermetallic compounds.

Welding also requires the use of clamps and jigs to prevent distortions of the panels during the thermal cycles. Residual stresses from welding may also create difficulties and limitations in structural applications of these panels.

Replacement of welding by adhesive bonding circumvents some of the difficulties associated with welding, but require careful surface preparation, tight tolerances, and time for the adhesive to cure. The use of adhesives may also be limited by environmental working conditions and requirements.

Under these circumstances, the aims and objective of this work is to extend the Opencell concept applicability to sandwich panels made of sheets from difficult or even impossible to weld materials. For this purpose, welding of the connection members will be replaced by a new joining by forming solution based on a mortise-and-tenon form-fit concept^{10–12} that was recently developed by the authors (Figure 2(b)).

The presentation starts by introducing the methods and procedures that were utilized to fabricate the connection members and to assemble the sandwich panels. A combined finite element and experimental work focused on the assembly of aluminum sandwich panels with the new proposed joining by forming process will then be utilized to validate the joints and to determine the required forces. The presentation finishes by showing an application of the new assembly procedure to produce aluminum – carbon fiber reinforced polymer sandwich panels that could only be assembled through welding.

Methods and procedures

Material and flow curve

The sandwich panels made use of EN AW 5754-H111 aluminum sheets with 5 mm thickness. The sheets were utilized in the ‘as-supplied’ condition and its mechanical characterization was carried out by

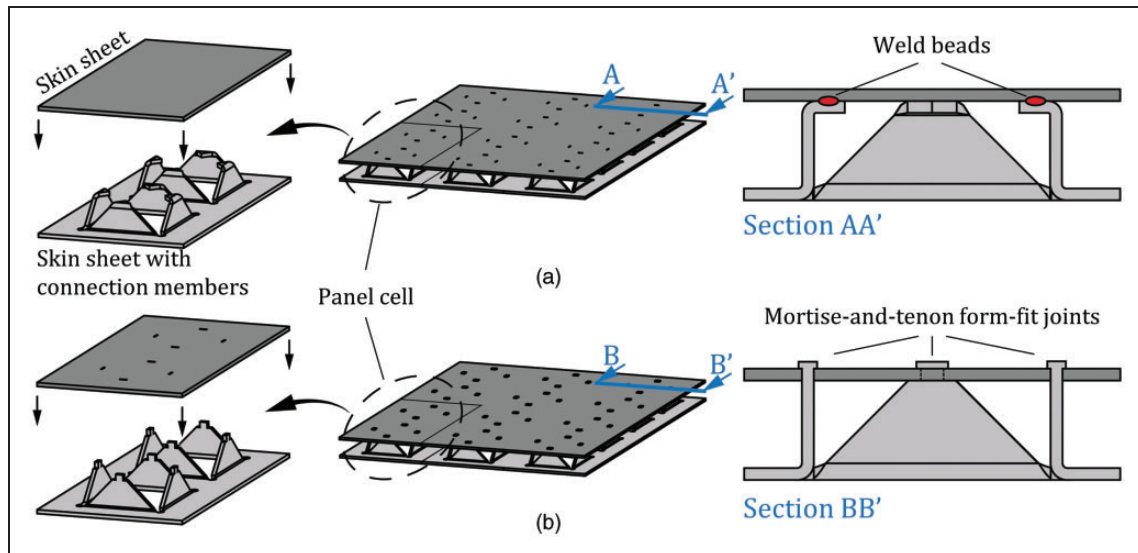


Figure 2. Schematic representation of all-metal sandwich panels based on the Opencell structure concept assembled through different joining technologies: (a) welding and (b) joining by forming. Cross-section details are provided for each type of joint.

Table 1. Mechanical properties of the EN AW 5754-H111 aluminum sheets obtained from tensile tests.

Modulus of elasticity, E (GPa)	Yield strength, σ_y (MPa)	Ultimate tensile strength, σ_{UTS} (MPa)	Elongation at break, A (%)	Anisotropy coefficient, r	Mean anisotropy coefficient, \bar{r}	Planar anisotropy coefficient, Δr
71.9	98.5	207.7	26.3	$r_0 = 0.62$ $r_{45} = 0.81$ $r_{90} = 0.73$	0.743	-0.135

means of standard tensile and stack compression tests.

The tensile tests were performed in accordance with the ASTM standard E8/E8M-16.¹³ The specimens were machined out from the supplied sheets at 0°, 45° and 90° with respect to the rolling direction and the results obtained for the modulus of elasticity, the yield strength, the ultimate tensile strength, the elongation at break, the anisotropy coefficients r_α , the average anisotropy \bar{r} and the planar anisotropy Δr coefficients, are summarized in Table 1

$$\bar{r} = \frac{r_0 + 2r_{45} + r_{90}}{4} \quad \Delta r = \frac{r_0 - 2r_{45} + r_{90}}{2} \quad (1)$$

The stack compression test specimens¹⁴ were prepared by piling-up three circular discs with 10 mm diameter that were also machined out from the supplied aluminum sheets. These tests were performed to obtain the material stress response for values of strain beyond plastic instability in tension because joining by forming subjects the sheets to high values of strain.

Both tensile and stack compression tests were carried out at ambient temperature and the average flow curve resulting from the entire set of experiments

(Figure 3) was approximated by the following Ludwik–Hollomon’s equation

$$\sigma = 325 \varepsilon^{0.18} (\text{MPa}) \quad (2)$$

Fabrication of the sandwich panels

The utilization of joining by forming, instead of welding, to fabricate sandwich panels with cores based on the Opencell concept, requires changes in the overall manufacturing route. The new proposed route is illustrated in Figure 4 and consists of three main operations that can be performed sequentially in a press equipped with a transfer system for transporting the sheets and moving them from one station to the other.

Firstly, the two adjoining sheets are punched to obtain the initial triangular-shaped blanks of the connecting members (Figure 4(a) – left) and the mortises with rectangular holes (Figure 4(a) – right). In case of the connecting members, an amount of material named as ‘the tenon’ is left at the edge of the triangular-shaped regions for later use in the assembly of the panel.

Punching to obtain the initial triangular-shaped blanks of the connecting members and the mortises

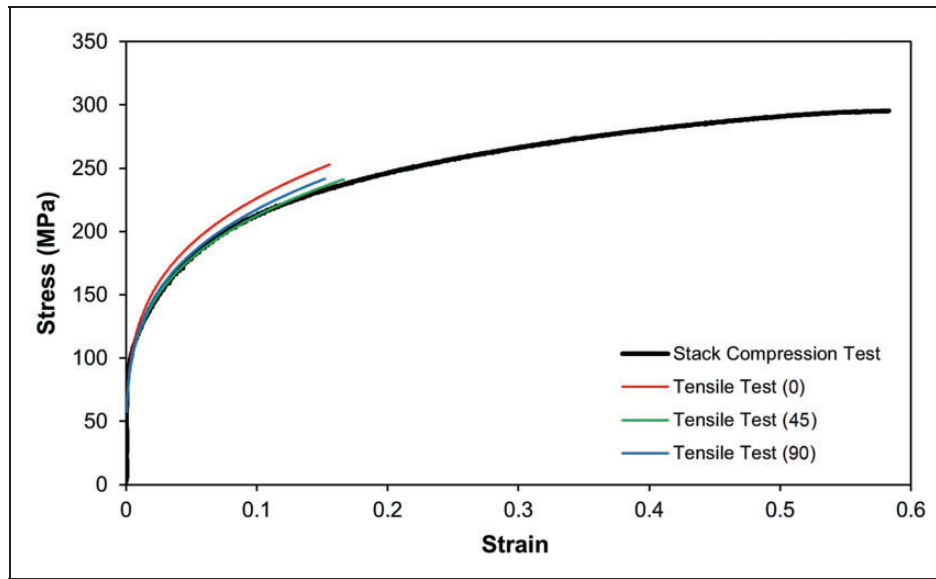


Figure 3. True stress vs. true strain curves for the entire set of tests performed on the EN AW 5754-H111 aluminum sheets.

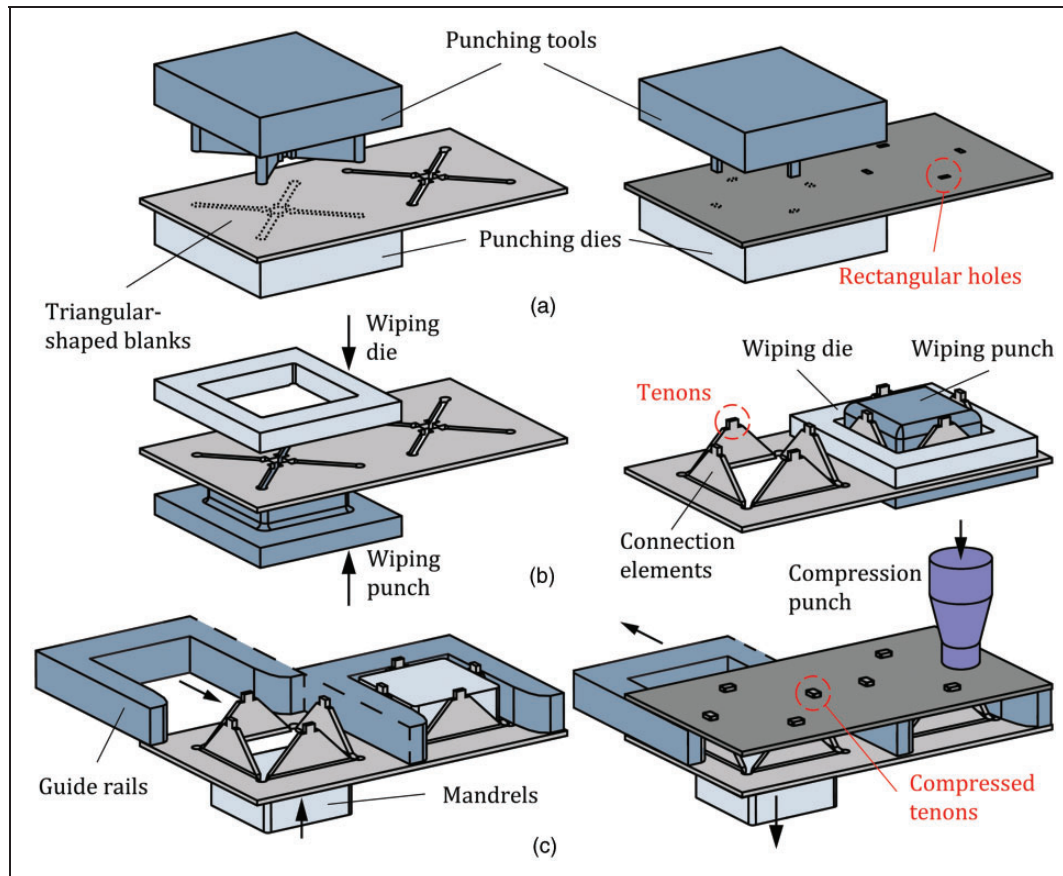


Figure 4. The proposed manufacturing route to produce sandwich panels based in the Opencell concept through joining by forming with a mortise-and-tenon concept: (a) punching, (b) bending, and (c) joining by forming.

with rectangular holes can also be replaced by laser or water jet cutting in case the first operation is to be performed before feeding the sheets into the press.

Secondly, the triangular-shaped blanks of the connecting members are bent along a straight line with a wiping tool (punch and die) to obtain ‘tab-style’

connection members perpendicular to their original sheet surfaces (Figure 4(b)).

Finally, the two sheets are placed in position on top of each other so that compression of the tenons in the direction perpendicular to the sheet thickness creates the mechanical interlocking (form-fit joints)

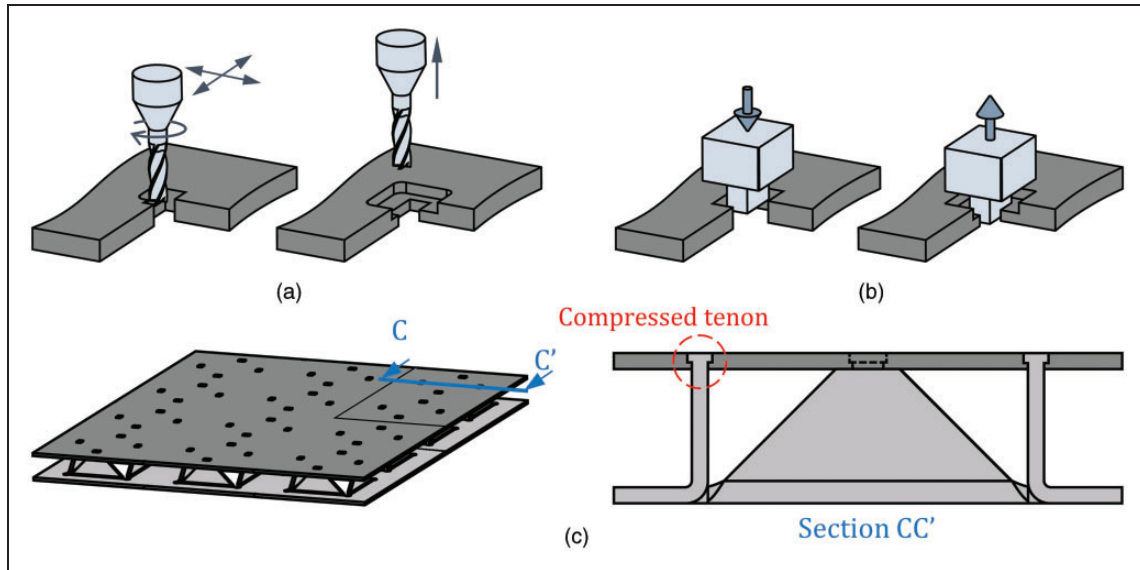


Figure 5. Counterbore mortises with rectangular stepped holes produced by combination of punching and (a) machining or (b) forging. The detail (c) shows a cross-section with a mechanical interlocking between the tenon and the mortise.

between the panel components (Figure 4(c)). Mandrels and guide rails are utilized to position the connection elements and to avoid failure by buckling during compression of the tenons with a flat punch.

As seen in Figure 4(c), the upper sheet surface contains material protrusions resulting from the joining by forming process. In case protrusions are not wanted as a result of aesthetic, dimensional or functional limitations, it is necessary to consider an intermediate operation (in-between the previously second and third operations) to produce counterbore (or countersunk) mortises (Figure 5). This intermediate operation can be done by machining (Figure 5(a)) or forging (Figure 5(b)).

In this work, authors combined punching with forging to produce the counterbore mortises with rectangular stepped holes (refer to the scheme shown in Figure 5(b)). The dimensions chosen for the rectangular punch hole and for the final counterbore mortise with rectangular stepped holes were derived for a previous work in joining by forming using the mortise-and-tenon concept.¹¹ Values are provided in Table 2.

Numerical modelling

The assembly of the aluminum sandwich panels through joining by forming was simulated with the in-house finite element computer program i-form.¹⁵ The program is based on the finite element flow formulation, which is built upon the weak form of the quasi-static force equilibrium equations

$$\int_V \sigma_{ij} \delta D_{ij} dV - \int_{S_t} t_i \delta u_i dS = 0 \tag{3}$$

In the above equation, σ_{ij} is the Cauchy stress tensor, D_{ij} is the rate of deformation tensor, t_i denotes the tractions applied on the boundary S_t with a normal with a vector of direction cosines given by n_j , and δu_i is an arbitrary variation in the velocity because the flow formulation is written in terms of velocities.

Decomposition of the Cauchy stress tensor σ_{ij} into a deviatoric tensor σ'_{ij} related to shape change and a hydrostatic tensor $\sigma_m = \delta_{ij} \sigma_{kk} / 3$ related to volume change, in which δ_{ij} denotes the Kronecker delta, allows rewriting the weak form of the quasi-static force equilibrium equations (3) as follows

$$\int_V \bar{\sigma} \delta \bar{\epsilon} dV + \int_V \sigma_m \delta \dot{\epsilon}_v dV - \int_{S_t} t_i \delta u_i dS = 0 \tag{4}$$

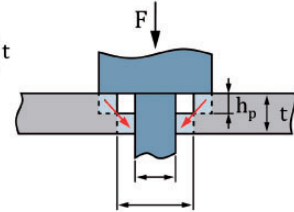
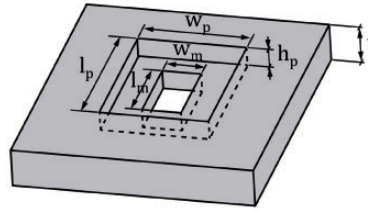
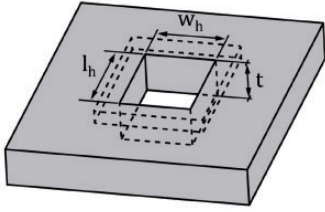
In the above equation $\dot{\epsilon}_v = D_v = \delta_{ij} D_{ij}$ is the volumetric rate of deformation and $\sigma'_{ij} \delta D_{ij} = \bar{\sigma} \delta \bar{\epsilon}$ is the increment of plastic power per unit of volume. The symbols $\bar{\sigma}$ and $\bar{\epsilon}$ denote the effective stress and strain rate. The computational approach to handle the second term in (4) is by relaxation of the incompressibility condition of the velocity field $\sigma_m = K \dot{\epsilon}_v$, where K is a large positive number known as the ‘penalty’.

Friction and contact between the different objects can be included in the formulation by rewriting (4) as follows

$$\begin{aligned} & \int_V \bar{\sigma} \delta \bar{\epsilon} dV + \int_V \sigma_m \delta \dot{\epsilon}_v dV - \int_{S_t} t_i \delta u_i dS \\ & + \int_{S_f} \left(\int_0^{u_r} \tau_f \delta u_r \right) dS + K_1 \sum_{c=1}^{N_c} g_n^c \delta g_n^c \\ & + K_2 \sum_{c=1}^{N_c} g_t^c \delta g_t^c = 0 \end{aligned} \tag{5}$$

Table 2. Geometry of the counterbore mortise with rectangular stepped holes.

Rectangular punched hole		Counterbore mortise with rectangular stepped holes				
w_h (mm)	l_h (mm)	w_p (mm)	l_p (mm)	h_p (mm)	w_m (mm)	l_m (mm)
6.5	11.2	8	12	2.5	5	10



The fourth term in (5) handles the contact with friction between deformable and rigid bodies, where the symbols, τ_f and u_r denote the friction shear stress and the relative sliding velocity on the contact interfaces S_f .

The fifth and sixth terms in (5) account for the interaction between deformable bodies by means of a two-pass contact search algorithm in which the N_c contact pairs are automatically extracted from the faces of the finite elements utilized in the discretization. The symbols g_n^c and g_t^c stand for the normal and tangential gap velocities in the contact pairs, which are penalized by large numbers K_1 and K_2 to avoid penetration. Details are given in Nielsen et al.¹⁵

In the present work the sixth term in (5) was not utilized because the deformable bodies were allowed to slide with friction along their contact interfaces.

The finite element models that were utilized to simulate the forging operation for producing the counterbore mortises with rectangular stepped holes and the joining by forming of the connection members to the sheets were built upon the unit cells that are schematically illustrated in Figure 6. As seen, the unit cells delimit the analysis to the vicinity of the plastically deforming regions with the remaining material of the sheet and connection member to be replaced by a fixed value displacement constraint.

The sheet and connection member within the unit cells were modelled as deformable objects and discretized by means of three-dimensional hexahedral elements. In contrast, the tools were modelled as rigid objects and discretized by means of contact-friction spatial triangular elements. Friction was modelled by means of the law of constant friction $\tau_f = mk$, where m is the friction factor and k is the shear flow stress. A value $m = 0.1$ was applied on the contact surfaces after checking the finite element predicted joining forces that best matched the experimental measurements.

Several remeshings were performed during the forging operation to cope with the progressive distortion of the elements and to allow the punch to move

downwards during the numerical simulation. No remeshings were necessary for the numerical simulation of the joining by forming operation.

Results and discussion

Deformation mechanics of the new joining by forming concept

Figures 7 and 8 provide a glimpse on material flow and effective strain distribution during the forging and joining by forming operations. As seen in Figure 7, the forging operation consists of a localized, partial compression of the sheet in the thickness direction to obtain a counterbore mortise with a rectangular stepped hole (refer to the velocity vectors in Figure 7). The highest values of effective strain are located at the transition between the inner wall and the rectangular step (with a fillet radius of approximately 0.3 mm) and are due to material being dragged and piled up by the punch along the thickness direction during sheet compression.

The predicted evolution of effective strain during joining by forming is given in Figure 8 and allows concluding that peak values with a magnitude like that obtained in forging are still located at the transition between the inner wall and the rectangular step. This means that the overall formability of the new proposed manufacturing route is controlled by the forging operation and not by the joining by forming operation that creates the mechanical interlocking (form-fit joint) between the connection member and the adjoining sheet.

The evolution of material flow in Figure 8 also allows concluding that the initial free height $h = 4.8$ mm and cross-sectional area $wl = 5 \times 10$ mm² of the tenon (refer to Figure 6) were chosen to ensure that its deformed geometry fits completely within the mortise, without protrusions above the sheet surface. This is confirmed by the photograph of the actual aluminum sandwich panel provided in Figure 9.

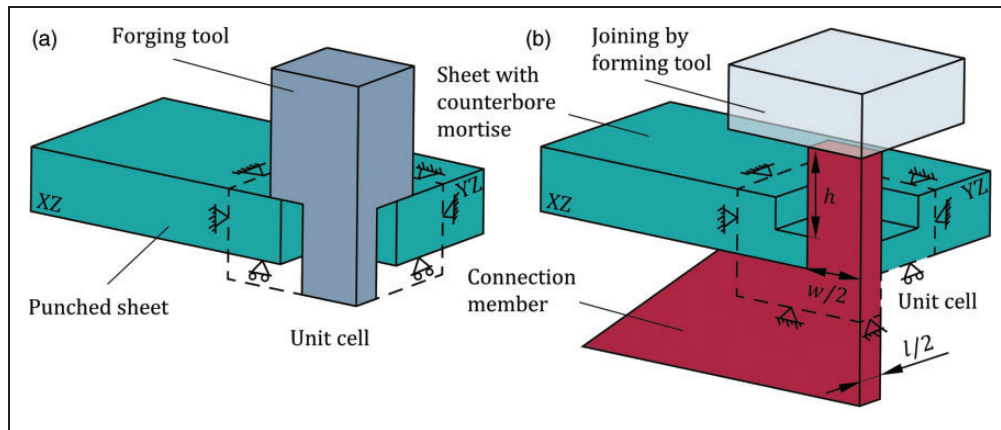


Figure 6. Finite element models of the unit cells that were utilized to simulate the assembly of the aluminum sandwich panels by means of the mortise-and-tenon concept: (a) Forging the punched sheet to obtain a counterbore mortise with a rectangular stepped hole and (b) joining by forming of the connection member to the adjoining sheet.

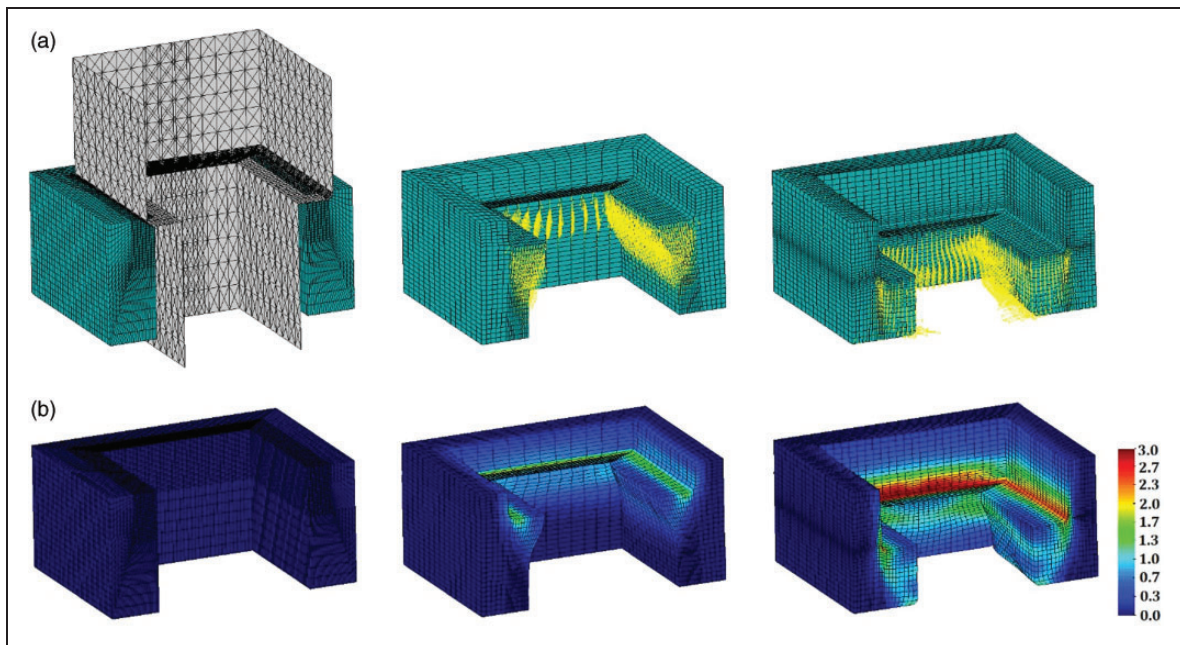


Figure 7. Finite element predicted evolutions of (a) material flow and (b) effective strain at the beginning, middle, and end stages of the forging operation to obtain a counterbore mortise with a rectangular stepped hole.

Figure 9 also contains photographs of the top sheet with the counterbore mortises with rectangular stepped holes (Figure 9(a) – left) and of the bottom sheet with the triangular-shaped connection members after bending along a straight line with a wiping tool (Figure 9(a) – right) that were utilized to fabricate the final sandwich panel shown in Figure 9(b).

Forging and joining forces

Unit cells like those shown in Figure 6 were utilized to obtain the experimental evolutions of the force with displacement in the forging and joining by forming operations (Figure 10). The evolution trends consist of two main regions labelled as ‘I’ and ‘II’. In region

‘I’ the force increases steeply with displacement because of the initial contact and accommodation of material with tooling. In region ‘II’ the force increases in a less pronounced way as the rectangular stepped hole and the free length of the connection member (i.e., the tenon) are progressively upset by compression.

A third region labelled as ‘III’, in which the force increases very rapidly with displacement, is observed in the graphic corresponding to the joining by forming operation (Figure 10(b)). Region ‘III’ is triggered when the mortise is close to being filled by the plastically deformed material of the tenon and the reason why there is no similar region in the force vs. displacement evolution of forging (Figure 9(a)) is because a

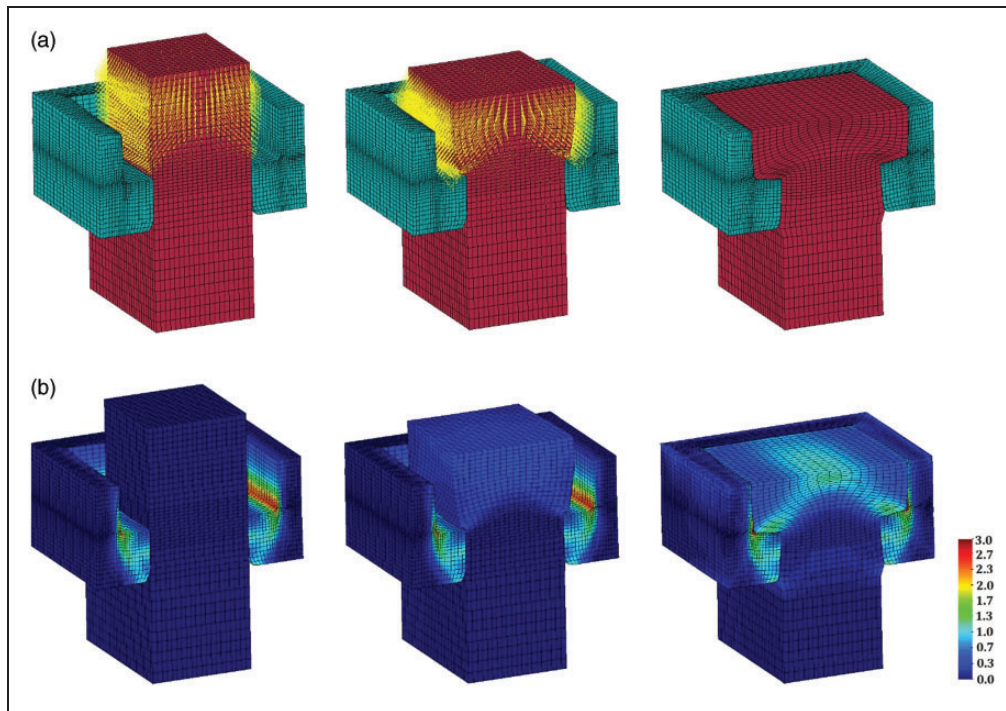


Figure 8. Finite element predicted evolutions of (a) material flow and (b) effective strain at the beginning, middle, and end stages of the joining by forming of the connection member to the adjoining sheet.

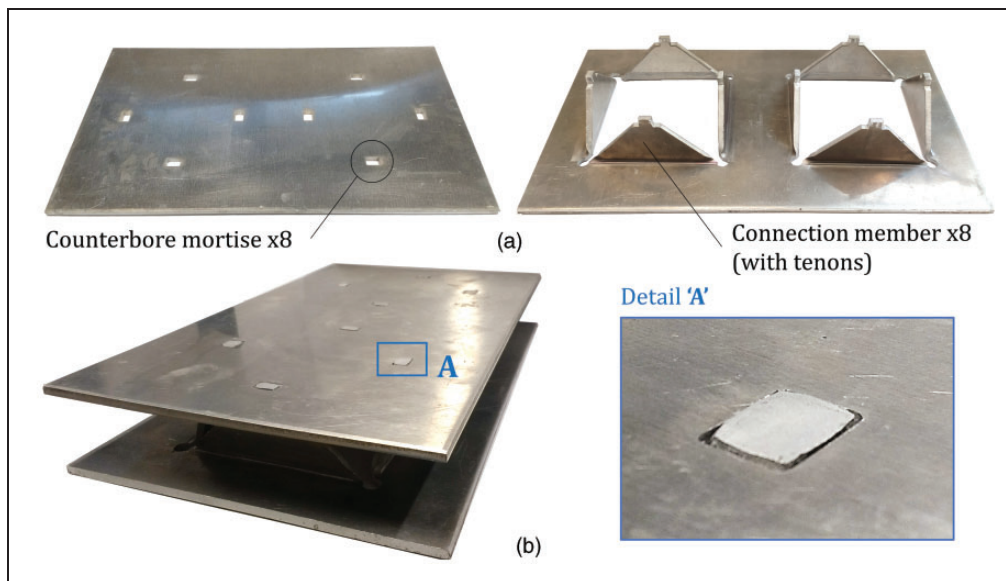


Figure 9. The new aluminum sandwich panel assembled through joining by forming: (a) top and bottom sheets showing the mortises and the connection elements of the core containing the tenons; (b) the final panel after assembly with a detail of the mechanical interlocking.

small clearance is left between the punch and the inner wall of the rectangular stepped hole of the mortise to facilitate positioning and entry of the tenon for the final assembly through joining by forming. This is also the reason why velocity vectors at the inner wall of the rectangular stepped hole are still pointing inward at the end of the forming operation (Figure 7).

The overall agreement between experimental and finite element predicted forces is good despite a small overestimation of the latter in regions 'II' and 'III' of the joining by forming operation (Figure 10(b)). This overestimation is attributed to the fact that the numerical model is stiffer than the experimental unit cell because the material located outside the dashed volumes of Figure 6, undergoing elastic deformation,

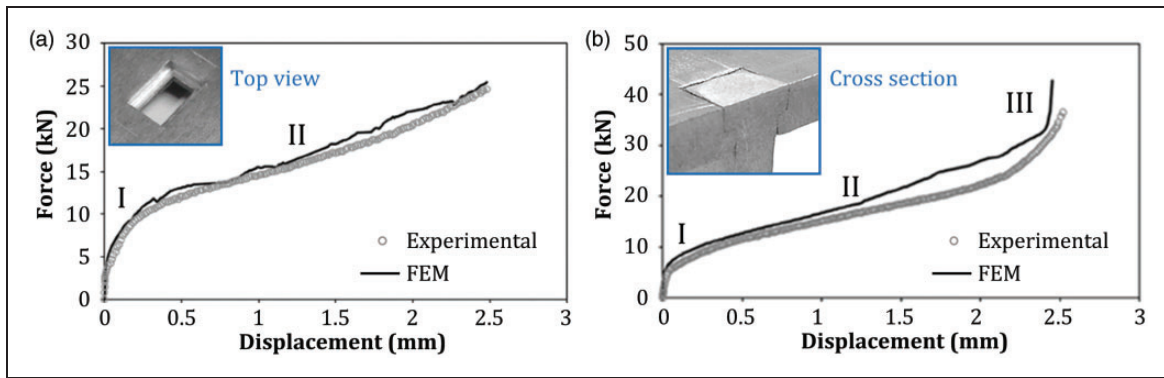


Figure 10. Experimental and finite element predicted evolution of the force vs. displacement for the unit cells that were utilized to replicate (a) the forging and (b) the joining by forming operations.

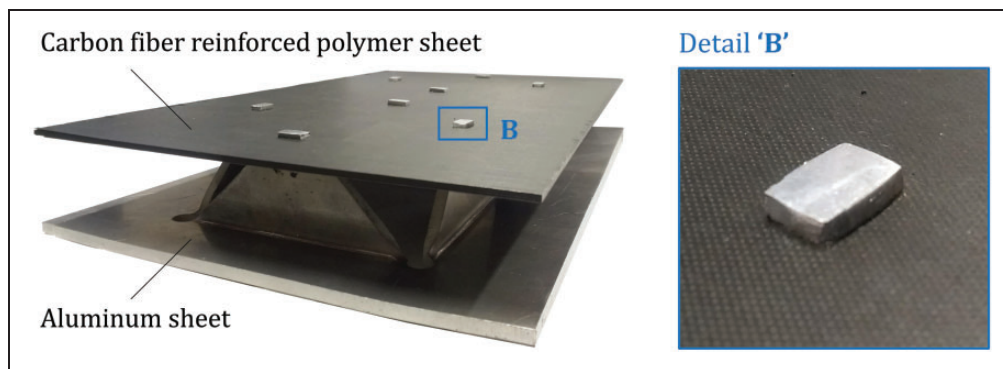


Figure 11. Full view and details of the aluminum-carbon fiber reinforced polymer sandwich panel assembled through joining by forming.

is treated as rigid and replaced by fixed displacement constraints. Still, a maximum force of 40 kN is estimated to assemble the aluminum sandwich panels through joining by forming in close agreement with the experimental measured value.

Extension to sandwich panels made from diss materials

This last section of the paper serves to demonstrate the potential of the new joining by forming solution to extend the Opencell concept to sandwich panels made from dissimilar materials that are impossible to weld or not recommended to be bonded with adhesive due to surface preparation, time to cure and environmental requirements.

The photographs included in Figure 11 show a full view and details of an aluminum – carbon fiber reinforced polymer sandwich panel assembled through joining by forming. As seen, the fabrication of this panel made use of a form-fit (mortise-and-tenon) joint with material protrusion of the tenon above the surface of the carbon fiber reinforced polymer sheet. However, other solutions based on the utilization of machining to fabricate the counterbore or countersunk mortises could have been employed to

obtain a flat sheet surface without material protrusions.

Conclusions

The manufacturing route to fabricate sandwich panels built upon the ‘Opencell’ structure concept was modified to replace welding or adhesive bonding by joining by forming, at ambient temperature. The experimental and numerical work combined with the analysis and interpretation of the results led to the following conclusions:

- The new manufacturing route comprises three main operations: punching (or cutting) the mortises and the connection members, bending the connection members and joining by forming the connection members to the adjoining sheets containing the mortises,
- Material protrusions above the sheet surfaces can be avoided if counterbore or countersunk mortises are used,
- The manufacturing route can be implemented in a transfer press to obtain high production rates,
- The assembly through joining by forming at ambient temperature prevents typical welding

limitations related to metallurgical changes, distortions, and residual stresses, as well as typical adhesive bonding limitations related to surface preparation, tight tolerances, and time for the adhesive to cure,

- The assembly through joining by forming is easy and very effective in case of difficult to weld sandwich panels made from aluminum sheets with medium-to-large thicknesses,
- The assembly of sandwich panels through joining by forming at ambient temperature enhances the environmental compliance of the overall manufacturing route and facilitates disassembly at the end of service life, allowing easy recyclability of the sheet materials.

Declaration of conflicting interests

The author(s) declared no potential conflicts of interest with respect to the research, authorship, and/or publication of this article.

Funding

The author(s) disclosed receipt of the following financial support for the research, authorship, and/or publication of this article: This study was supported by Fundação para a Ciência e a Tecnologia of Portugal and IDMEC under LAETA-UIDB/50022/2020.

ORCID iD

PAF Martins  <https://orcid.org/0000-0002-2630-4593>

References

1. Thomsen OT. Sandwich materials for wind turbine blades – present and future. *J Sandw Struct Mater* 2009; 11: 7–26.
2. Palkowski H and Carradó A. Metal-polymer-metal laminates for lightweight application. *Key Eng Mater* 2016; 684: 323–334.
3. Mills NJ. Sandwich panel case study. In: *Polymer foams handbook*. Oxford: Butterworth-Heinemann, 2007, pp.425–447.
4. Partridge IK, Cartie DDR and Bonnington T. Manufacture and performance of z-pinned composites. In: Advani S and Shonaika G (eds) *Advanced polymeric materials: structure–property relationships*. Boca Raton, FL: CRC Press, 2003, pp.103–138.
5. Zaid NZM, Rejab MRM and Mohamed NAN. Sandwich structure based on corrugated-core: a review. In: *ICMER 2015 – 3rd international conference of mechanical engineering research, MATEC Web of Conferences* 2016.
6. Abbadi A, Koutsawa Y, Carmasol A, et al. Experimental and numerical characterization of honeycomb sandwich composite panels. *Simul Model Pract Theory* 2009; 17: 1533–1547.
7. Säynäjäkangas J and Taulavuori T. A review in design and manufacturing of stainless steel sandwich panels. *Stainless Steel World* 2004; October: 55–59.
8. Valente A, Taulavuori T, Säynäjäkangas J, et al. *Panel structure*. Outokumpu Oyj, WO/2009/034226, 2009.
9. Valente A, Sirén M and Säynäjäkangas J. Design, manufacture and properties of the novel Opencell metal sandwich panel. *Hitsaus Tekniikka* 2010; 4: 27–34.
10. Bragança IMF, Silva CMA, Alves LM, et al. Joining sheets perpendicular to one other by sheet-bulk metal forming. *Int J Adv Manuf Technol* 2017; 89: 77–86.
11. Silva CMA, Bragança IMF, Alves LM, et al. Two-stage joining of sheets perpendicular to one another by sheet-bulk forming. *J Mater Process Technol* 2018; 253: 109–120.
12. Silva DFM, Silva CMA, Bragança IMF, et al. On the performance of thin-walled crash boxes joined by forming. *Materials* 2018; 11: 1118
13. ASTM E8/E8M. *Standard test methods for tension testing of metallic materials*. West Conshohocken, PA: ASTM International, 2013.
14. Alves LM, Nielsen CV and Martins PAF. Revisiting the fundamentals and capabilities of the stack compression test. *Exp Mech* 2011; 51: 1565–1572.
15. Nielsen CV, Zhang W, Alves LM, et al. Coupled finite element flow formulation In: Davim JP (ed) *Modelling of thermo-electro-mechanical manufacturing processes with applications in metal forming and resistance welding*. New York: Springer, 2013, pp.11–35.